Bulletin of Engineering Geology and the Environment
https://doi.org/10.1007/s10064-020-01903-x

ORIGINAL PAPER

Stability analysis of slopes using the vector sum numerical manifold method

Yongtao Yang[1] · Wenan Wu[1,2] · Hong Zheng[1,3]

Received: 7 November 2019 / Accepted: 25 June 2020

Abstract

The NMM (numerical manifold method) has shown its ability to solve continuum and discontinuum engineering problems in the same framework. In the present paper, the vector sum NMM (VSNMM) is proposed to investigate the stability of slopes. With the (vector sum numerical manifold method) VSNMM, the FOSs (factors of safety) of slopes are obtained using the real stress fields of the slopes. Compared with the limit equilibrium methods, the deformation and stress field of a slope can be obtained using the VSNMM. Besides, the computational cost of the VSNMM is much less than that of the strength reduction numerical manifold method (SRNMM), since only one elasto-plastic analysis is needed in the VSNMM, while a series of elasto-plastic analyses is needed in the SRNMM. Based on the VSNMM, the stability analyses of two slopes including a homogeneous slope and an inhomogeneous slope with three different materials are conducted. The numerical results based on the two slopes show that the VSNMM can accurately calculate the FOSs of the slopes.

Keywords Numerical manifold method (NMM) · Vector sum method (VSM) · Strength reduction method · Slope stability

Introduction

Stability analysis of slopes is still a very attractive topic in the geotechnical engineering. To evaluate the stability of slopes, several type of methods such as the limit analysis methods, the limit equilibrium methods (LEMs), and the numerical methods have been proposed (Chen 2003). However, the LEMs and the numerical methods, to the best knowledge of the authors, are most widely used.

Although the LEMs (Morgenstern and Price 1965; Sun et al. 2017) including the Bishop method, the Morgenstern–Price method, the Spence method, and the Sarma method are simple to be used by geotechnical engineers, they suffer from some drawbacks. For example, the sliding body of the slope is assumed as a rigid body. Hence, the deformation of the slope cannot be considered. Furthermore, in some LEMs the distribution of internal forces between adjacent slices has to be assumed (Griffiths and Lane 1999).

To avoid the drawbacks of the LEMs, many numerical methods (Zienkiewicz and Taylor 2000; Zhuang et al. 2012; Rabczuk et al. 2010; Yang et al. 2017, 2018a, c; Yang and Zheng 2016, 2017; Xu et al. 2020; Wu et al. 2020) have been proposed. The FEM (abbreviated form for the finite element method) can be considered a representative. To investigate the stability of slopes, the limit equilibrium concepts have been implemented into the FEM (Fredlund and Scoular 1999). In the limit equilibrium FEM, there is no need to slice the sliding body. Furthermore, the stress field and deformation of the sliding body of the slope can be easily obtained. However, the meshes in the FEM have to be carefully deployed, since the FE meshes have to match the physical meshes (material interfaces, fracture faces, joints, and so on) (Yang et al. 2017). For very complex problems, such as the soil-rock-mixtures presented in (Chen et al. 2018, 2019; Yang et al. 2019d, 2019c, 2020a, 2020c), it is very difficult to avoid the generation of poor quality meshes. Note that accuracy assessed from some iso-parametric elements is very sensitive to the quality of the FE meshes (Lee and Bathe 1993).

✉ Yongtao Yang
ytyang@whrsm.ac.cn

1 State Key Laboratory of Geomechanics and Geotechnical Engineering, Institute of Rock and Soil Mechanics, Chinese Academy of Sciences, Wuhan 430071, China

2 University of Chinese Academy of Sciences, Beijing 100049, China

3 Key Laboratory of Urban Security and Disaster Engineering, Ministry of Education, Beijing University of Technology, Beijing 100124, China

Published online: 12 August 2020

Alternatively, the NMM (numerical manifold method) is proposed to overcome the difficulty arising in the FEM (Shi 1991; Zheng and Yang, 2017; Yang et al. 2020b, 2020d). In the NMM, there is no need for the mathematical meshes to match the physical meshes. To be more specifically, regular meshes which perform better than distorted meshes can consistently be adopted. Additionally, the discontinuity can be easily captured in the NMM without introducing any additional functions, such as the Heaviside functions used in the XFEM (Mohammadnejad and Khoei 2013). Due to these attractive characteristics, the NMM has been proposed for many different types of engineering problems (Wu and Wong 2012; Yang et al. 2016, 2018b, 2019a, 2019b). However, application of the NMM for the analysis of slope stability is still very limited.

In order to obtain the FOSs (factors of safety) of the slopes, other techniques such as the strength reduction method (SRM) (Matsui and San 1992; Zheng et al. 2002, 2005) and the vector sum method (VSM) (Guo et al. 2011) should be implemented into the numerical methods. In regard to the SRM, a series of elasto-plastic analyses with a numerical method should be conducted. Once the slope is exactly in a failure verge state, the processes of elasto-plastic analysis are terminated, and the FOS of the slope can be obtained. However, the elasto-plastic analysis is usually time-consuming. Hence, the computational cost of the SRM cannot be neglected. In regard to the VSM, only one elasto-plastic analysis is needed. According to the real/current stress field assessed from a numerical method, the FOS of the slope can be calculated directly using the VSM.

In the present work, a vector sum numerical manifold method (VSNMM) is proposed. The VSM is implemented into the NMM to predict the FOSs of the slopes. Based on the proposed VSNMM, stability analyses of two slopes including a homogeneous slope and an inhomogeneous slope with three materials are conducted. The results show that the VSNMM can accurately calculate the FOSs of the slopes. The proposed VSNMM deserves a further investigation.

Brief the numerical manifold method

Some concepts in the NMM

In this section, the basic concepts in the numerical manifold method (NMM) are introduced, although they have been presented in many literature (Zheng and Xu 2014). For the convenience of description, we adopt Fig. 1 as an example.

There are two important cover systems (CSs) in the NMM, which are mathematical CS and physical CS. The mathematical CS is usually generated from a series of mathematical patches (MPs). A MP (such as the MP_1 and the MP_2) is generated through several rectangular meshes having a mutual node. The physical CS is usually generated from a series of physical patches (PPs). The PPs are obtained through slicing the MPs with the physical meshes (PMs). Cutting MP_2 using PMs will yield PP_2; cutting MP_3 using PMs will yield PP_3 and PP_4. Note that a NMM node will be attached to a PP. For example, GN_2^P is attached to PP_2. The MEs (manifold elements) are the mutual parts for four neighboring PPs.

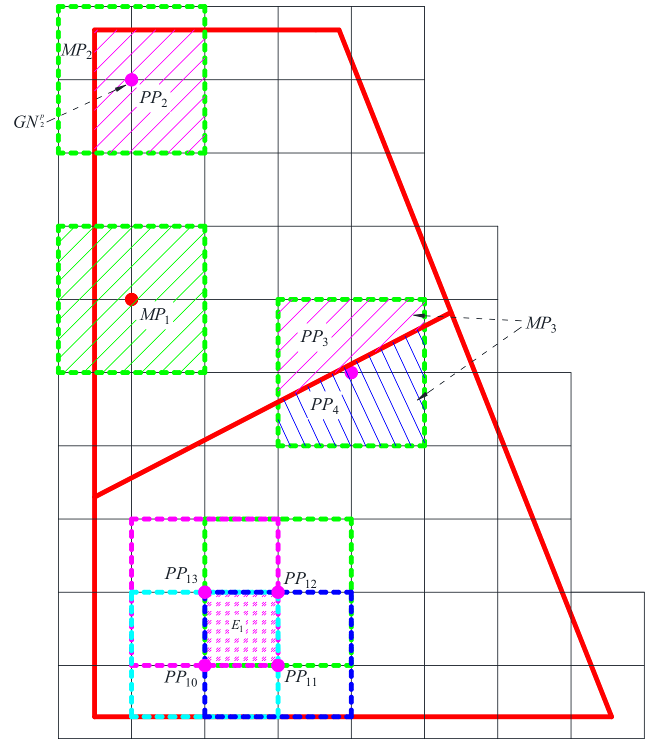

Fig. 1 Some basic concepts in the NMM

Over a ME, the global displacement function $\boldsymbol{u}^h(\boldsymbol{x})$ can be obtained using Eq. (1).

$$\boldsymbol{u}^h(\boldsymbol{x}) = \sum_{k=1}^{4} w_k(\boldsymbol{x})\boldsymbol{u}_k(\boldsymbol{x}) \tag{1}$$

in which $w_k(x)$ and $\boldsymbol{u}_k(x)$ separately represent the weight function and cover function.

Since rectangular meshes are used to form the MPs and the mathematical CS, the shape function of the four-node quadrilateral element can then be conveniently adopted to construct

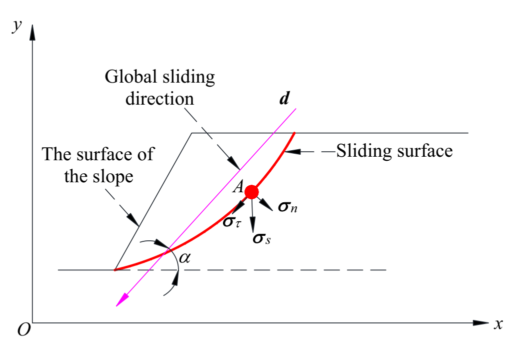

Fig. 2 A sketch for the potential sliding surface of a simple slope

Fig. 3 A homogeneous slope and its three discretized models. **a** A sketch for the slope. **b** Model A (1247 MEs, 1336 PPs). **c** Model B (2744 MEs, 2875 PPs). **d** Model C (7761 MEs, 7982 PPs)

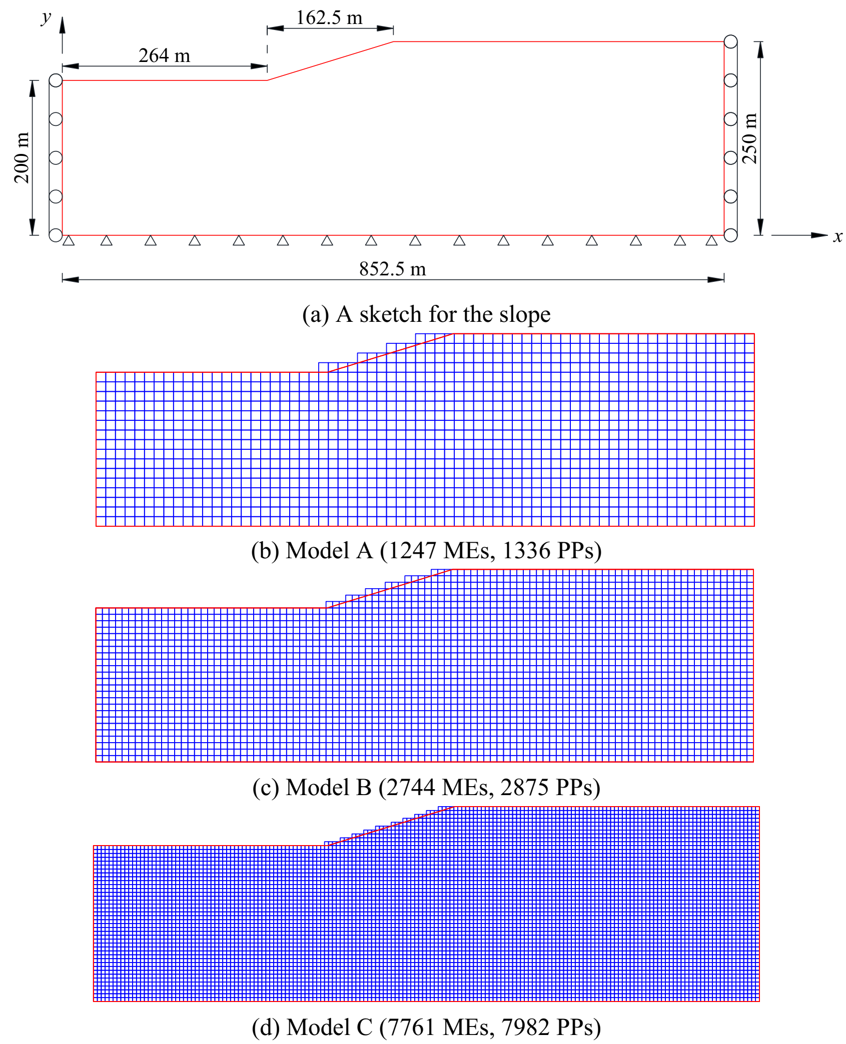

$w_k(\boldsymbol{x})$. Furthermore, to avoid the linear dependent problem, constant is adopted to construct the $\boldsymbol{u}_k(\boldsymbol{x})$. The formulation for $\boldsymbol{u}^h(\boldsymbol{x})$ can then be formulated as:

$$\boldsymbol{u}^h(\boldsymbol{x}) = \boldsymbol{N}\boldsymbol{d} \tag{2}$$

in which d and N separately represent the vector of DOFs and matrix of shape function.

The discretized form

In regard to elasto-plastic problems, the corresponding weak form can be defined as

$$\int_\Omega (\delta\varepsilon)^{\mathrm{T}} \boldsymbol{D}^{ep} \varepsilon \mathrm{d}\Omega = \int_\Omega \delta \boldsymbol{u}^{\mathrm{T}} \boldsymbol{b} \mathrm{d}\Omega + \int_{\Gamma_t} \delta \boldsymbol{u}^{\mathrm{T}} \boldsymbol{t} \mathrm{d}\Gamma, \tag{3}$$

in which δu represents the virtual displacement, Ω represents the problem domain, $\boldsymbol{b}$ represents the body force, ε represents the strain, $\boldsymbol{D}^{ep}$ represents the elasto-plastic matrix, and $\bar{t}$ represents the specified traction defined on traction boundary Γ_t.

Substitution of Eq. (2) into Eq. (3), the system equations in the discretized form will be obtained and expressed as:

$$\boldsymbol{K}\boldsymbol{d} = \boldsymbol{f}, \tag{4}$$

in which K and f are the global stiffness matrix and the vector of global nodal force, respectively:

$$\boldsymbol{K} = \int_\Omega \boldsymbol{B}^{\mathrm{T}} \boldsymbol{D}^{ep} \boldsymbol{B} d\Omega, \quad \boldsymbol{f} = \int_\Omega \boldsymbol{N}^{\mathrm{T}} \boldsymbol{b} d\Omega + \int_{\Gamma_t} \boldsymbol{N}^{\mathrm{T}} \boldsymbol{t} d\Gamma \tag{5}$$

Table 1 Properties of material used in Validation example: A homogeneous slope section

Parameter	Magnitude
Young's modulus (Pa)	80×10^6
Poisson's ratio	0.43
Angle of internal friction(°)	11.31
Cohesion(Pa)	58.86×10^3
Unit weight (kN/m^3)	19.62

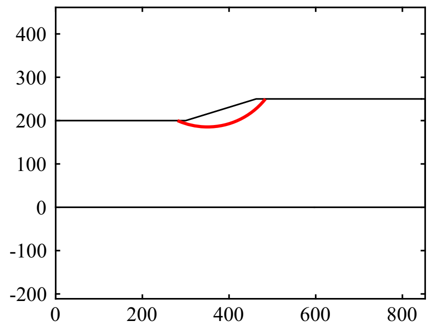

Fig. 4 Location of potential sliding surface for the homogeneous slope (unit: m)

in which

$$\boldsymbol{B} = \boldsymbol{L}_d\boldsymbol{N}, \quad \boldsymbol{L}_d^{\mathrm{T}} = \begin{bmatrix} \frac{\partial}{\partial x} & 0 & \frac{\partial}{\partial y} \\ 0 & \frac{\partial}{\partial y} & \frac{\partial}{\partial x} \end{bmatrix} \tag{6}$$

The vector sum method

The vector sum method (VSM) was firstly proposed by Ge et al. (Ge 2010; Guo et al. 2011) to investigate slope stability. According to the vector feature of forces, the FOS in the VSM is expressed as the ratio of vector sum of ultimate resistance forces to those of driving forces projected to the potential global sliding direction. To describe the basic idea of the VSM, we take Fig. 2 as an example.

In Fig. 2, $\boldsymbol{d}$ represents the potential global sliding direction, α represents the included angle between $\boldsymbol{d}$ and x-axis. σ_s, σ_τ, and σ_n separately represent the stress vector, the normal stress vector, and the shear stress vector at point A on the potential sliding surface S. Formulations for σ_s, σ_τ, and σ_n can be expressed as

$$\boldsymbol{\sigma}_s = \boldsymbol{\sigma}\bullet\boldsymbol{n} \tag{7}$$

$$\boldsymbol{\sigma}_n = (\boldsymbol{\sigma}_s\bullet\boldsymbol{n})\boldsymbol{n} \tag{8}$$

$$\boldsymbol{\sigma}_\tau = \boldsymbol{\sigma}_s - \boldsymbol{\sigma}_n \tag{9}$$

in which σ and n separately represents the stress tensor and unit normal vector at point A.

Table 2 The FOS of the slope assessed from the VSNMM

Discretized models	FOS
Model A	1.395
Model B	1.375
Model C	1.367
Reference solution	1.360

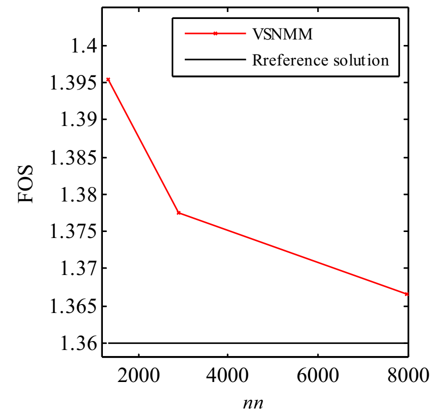

Fig. 5 Convergence of solution for the stability analysis of the homogeneous slope

The normal stress at A applied by the bedrock is

$$\boldsymbol{\sigma}_n^{'} = -\boldsymbol{\sigma}_n \tag{10}$$

The FOS in the VSM can be expressed in the following form:

$$F = \frac{R}{T} \tag{11}$$

where

$$T = \int_S (\boldsymbol{\sigma}_s\boldsymbol{d})\mathrm{d}S \tag{12}$$

$$R = \int_S \boldsymbol{\sigma}_s^{'}(-\boldsymbol{d})\mathrm{d}S \tag{13}$$

in which $\boldsymbol{\sigma}_s^{'}$ represents the maximum anti-sliding stress vector. T and R separately represent the total sliding force and anti-sliding force projected to d.

The maximum anti-shear stress $\boldsymbol{\sigma}_\tau^{'}$ at point A is formulated according to the M-C yield criterion (Zheng et al. 2005; Owen and Hinton 1980) and expresses as

$$\boldsymbol{\sigma}_\tau^{'} = -(c - \sigma_n \tan\phi)\boldsymbol{d}_r \tag{14}$$

in which c represents the strength of cohesion, ϕ represents the angle of internal friction, and d_r represents the unit shear stress direction.

The formulation of $\boldsymbol{\sigma}_s^{'}$ is expressed as

$$\boldsymbol{\sigma}_s^{'} = \boldsymbol{\sigma}_\tau^{'} + \boldsymbol{\sigma}_n^{'} \tag{15}$$

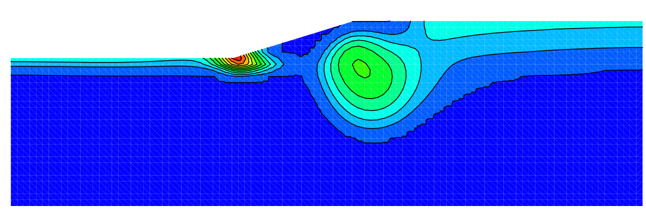

Fig. 6 Equivalent plastic strain contours of the homogeneous slope based on the SRNMM using the Model B ($FOS^i = 1.36$)

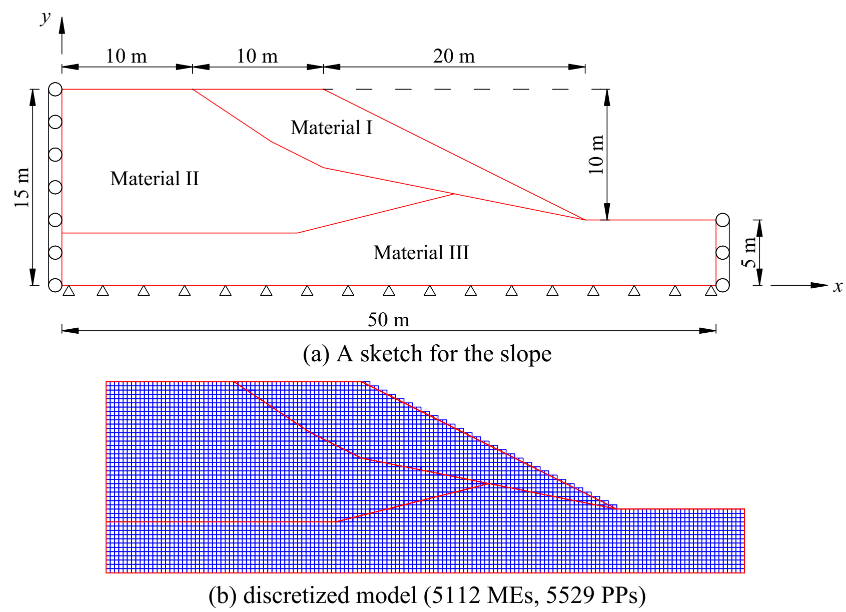

Fig. 7 An inhomogeneous slope and its discretized model. **a** A sketch for the slope. **b** discretized model (5112 MEs, 5529 PPs)

The formulation of d is expressed as (Guo et al. 2011)

$$\boldsymbol{d} = \frac{-\int_S (c - \sigma_n \tan\phi) \boldsymbol{d}_r \mathrm{d}S}{\left\| \int_S (c - \sigma_n \tan\phi) \boldsymbol{d}_r \mathrm{d}S \right\|} \tag{16}$$

As discussed in (Guo et al. 2011), the VSM is very similar to those traditional methods. Note that each method has its own advantages and disadvantages. The LEMs are easy to be implemented and have been adopted by geotechnical engineers for many years. However, the deformation and stress field of the slope cannot be calculated in the LEMs. More importantly, the stress distribution on the interface of two neighboring slices has to be assumed. Although the critical failure surface (sliding surface) in the SRM can be located automatically, it will take relatively a very long time to obtain the FOS of the slope, since a series of elasto-plastic analyses which are usually time-consuming should be carried out in the SRM. According to the vector characteristics of the forces, the VSM is able to obtain the FOSs using the real/current stress fields of the slopes (only one elasto-plastic analysis is needed). However, the failure surface should be located in the VSM.

Table 3 Properties of material used in An inhomogeneous slope section

Physical parameters	Magnitude		
	Material I	Material II	Material III
Young's modulus(Pa)	200×10^6	250×10^6	300×10^6
Poisson's ratio	0.35	0.30	0.28
Angel of internal friction(°)	20	25	26
Cohesion (KPa)	12.38	15	20
Unit weight (Kg/m^3)	20	22	23

Numerical tests

Two numerical tests are adopted to evaluate the performance of the VSNMM. The following methods will be adopted in this section, which are:

(1) VSNMM (vector sum numerical manifold method), the vector sum method is implemented into the numerical manifold method to investigate the stability of the slope.
(2) SRNMM (strength reduction numerical manifold method), the strength reduction method is implemented into the NMM to investigate the stability of the slope. In SRNMM, the potential sliding surface can be obtained automatically.
(3) VSBEM (vector sum boundary element method) (Deng et al. 2010). the vector sum method is implemented into the boundary element method to investigate the stability of the slope.
(4) Morgenstern–Price method, one of the LEMs (Morgenstern and Price 1965).

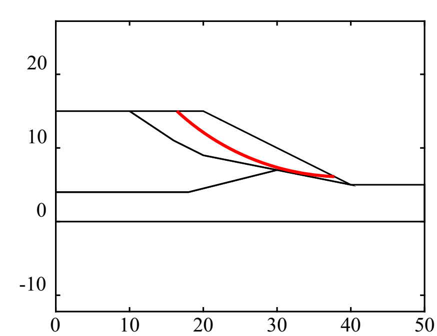

Fig. 8 Location of potential sliding surface based on the Morgenstern–Price method (unit: m)

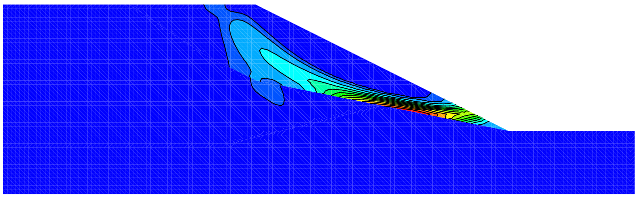

Fig. 9 Equivalent plastic strain contour of the inhomogeneous slope based on the SRNMM ($FOS^i = 1.66$)

For the convenience of comparison, the potential sliding surfaces used in the VSNMM and VSBEM to predict the FOSs of the slopes are based on the sliding surfaces obtained from the Morgenstern–Price method.

Validation example: A homogeneous slope

As the first example, a homogeneous slope subjected to gravity load is considered. The dimension and boundary conditions are shown in Fig. 3(a). The parameters used for this example are listed in Table 1. To investigate the convergence of solution assessed from the VSNMM, three discretized models, namely, Model A, Model B, and Model C (Fig. 3b–d) are adopted. Due to the lack of analytical solution for this problem, the Morgenstern–Price method is adopted to obtain the reference solution.

The location of potential sliding surface for the homogeneous slope based on the Morgenstern–Price method is plotted in Fig. 4.

The FOS of the slope assessed from the VSNMM using different discretized models are list together in Table 2. For the purpose of observation, the results presented in Table 2 are also plotted in Fig. 5. As can be seen in Fig. 5, the FOS of the slope approaches to the reference solutions as the number of physical patches increases.

The SRNMM is also adopted to predict the FOS. The equivalent plastic strain contour (EPSC) of the homogeneous slope using Model B is plotted in Fig. 6. As can be seen in Fig. 6, the FOS assessed from the SRNMM is 1.36, which is close to that assessed from the VSNMM. However, the FOS assessed from the SRNMM is obtained by solving a series of elasto-plastic problems. Note that this process is usually very time-consuming.

In addition, the FOS of the slope assessed from the VSBEM is 1.410 (Deng et al. 2010). Obviously, the results from the VSNMM are better than those from the VSBEM, even the Model A is used.

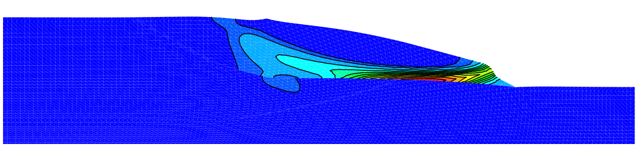

Fig. 10 Equivalent plastic strain contour of the inhomogeneous slope plotted on the deformed model ($FOS^i = 1.66$)

Table 4 The FOSs assessed from different methods for the example presented in An inhomogeneous slope section

Methods	FOS
Morgenstern-Price method	1.652
SRNMM	1.660
VSNMM	1.659

An inhomogeneous slope

In this section, an inhomogeneous slope with three materials is investigated. Figure 7(a) presents the dimension and boundary conditions for this slope. The discretized model is shown in Fig. 7(b). The computational parameters of the three materials are listed together in Table 3. The location of potential sliding surface based on the Morgenstern–Price method is presented in Fig. 8. The EPSC of the inhomogeneous slope based on the SRNMM is presented in Fig. 9. In addition, the EPSC of the inhomogeneous slope is also plotted on the deformed model, as shown in Fig. 10. As can be seen in Fig. 9 and Fig. 10, when the strength reduction factor (FOS^i) is 1.66, a continuous plastic zone which passes from the toe of the slope to the top of the slope is formed. For comparison, the FOS of this slope based on different methods are presented in Table 4. As can be seen in Table 4, FOSs of the slope assessed from the SRNMM and the VSNMM are almost the same. Furthermore, the FOSs assessed from the SRNMM and the VSNMM agree well with those from the Morgenstern–Price method.

Conclusions

In this study, a vector sum numerical manifold method (VSNMM) is developed to investigate the slope stability. With the VSNMM, the stability of two slopes is investigated. According to the results, we can draw the following conclusions:

(a) In the first example, a homogeneous slope is considered. The numerical results show that the FOS (factor of safety) of the slope assessed from the VSNMM approach to the reference solution as the number of physical patches increases. In addition, the FOS assessed from the VSNMM agrees well with that from the SRNMM, and better than that from the VSBEM.

(b) In the second example, an inhomogeneous slope with three different materials is considered. The numerical results show that the FOS assessed from the VSNMM agrees well with those from the SRNMM and the Morgenstern–Price method.

Only a two-dimensional static analysis is considered in the present paper. However, all the real geotechnical problems are in three-dimensional space. Hence, it is necessary to develop a numerical model that can consider three-dimensional problems. In our future work, we will extend our numerical model for three-dimensional static and dynamic problems. In addition, the risk analysis (Luo and Bathurst 2018) will also be conducted, and the random field will be implemented into the proposed numerical model to consider the spatial variability of soil.

Funding information This study is supported by the Youth Innovation Promotion Association CAS, under the grant no. 2020327; and the National Natural Science Foundation of China, under the grant nos. 51609240, 11172313, and 51538001.

References

Chen Z (2003) Earth slope stability analysis-theory, method and programs. China Water Power Press, Beijing

Chen L, Yang YT, Zheng H (2018) Numerical study of soil-rock mixture: generation of random aggregate structure. Science China Technol Sci 61:359–369

Chen T, Yang YT, Zheng H, Wu ZJ (2019) Numerical determination of the effective permeability coefficient of soil-rock mixtures using the numerical manifold method. Int J Numer Anal Methods Geomech 43(1):381–414

Deng Q, Guo M, Li C, Ge X (2010) Vector sum method for slope stability analysis based on boundary element method. Rock and Soil Mechanics 31(6):1971–1976

Fredlund DG, Scoular REG (1999) Using limit equilibrium concepts in finite element slope stability analysis[C]//Int. Symp. on Slope Stability Engineering, Matsuyama, pp 31–47

Ge XR (2010) A new method for anti-sliding stability analysis — basic principle of vector sum analysis method and its application[C] Proceedings of the 11th National Rock Mechanics and Engineering Conference. Wuhan: Hubei Science and Technology Press: 26–44

Griffiths DV, Lane P (1999) A slope stability analysis by finite elements. Géotechnique 49(3):387–403

Guo MW, Ge XR, Wang SL (2011) Slope stability analysis under seismic load by vector sum analysis method. J Rock Mech Geotech Eng 3(3):282–288

Lee NS, Bathe KJ (1993) Effects of element distortions on the performance of isoparametric elements. Int J Numer Methods Eng 36(20): 3553–3576

Luo N, Bathurst RJ (2018) Probabilistic analysis of reinforced slopes using RFEM and considering spatial variability of frictional soil properties due to compaction. Georisk: Assessment and Management of Risk for Engineered Systems and Geohazards 12(2):87–108

Matsui T, San KC (1992) Finite element slope stability analysis by shear strength reduction technique. Soils Foundations 32(1):59–70

Mohammadnejad T, Khoei AR (2013) An extended finite element method for hydraulic fracture propagation in deformable porous media with the cohesive crack model. Finite Elem Anal Des 73:77–95

Morgenstern NR, Price VE (1965) The analysis of the stability of general slip surface. Géotechnique 15(1):79–93

Owen DRJ, Hinton E (1980) Finite elements in plasticity: theory and practice. Pineridge Press, Swansea

Rabczuk T, Zi G, Bordas S, Nguyen-Xuan H (2010) A simple and robust three-dimensional cracking-particle method without enrichment. Comput Methods Appl Mech Eng 199:2437–2455

Shi GH (1991) Manifold method of material analysis. In: Proceedings of the Transactions of the Ninth Army Conference on Applied Mathematics and Computing: 57–76

Sun GH, Yang YT, Cheng SG, Zheng H (2017) Phreatic line calculation and stability analysis of slopes under the combined effect of reservoir water level fluctuations and rainfall. Can Geotech J 54(5):631–645

Wu Z, Wong LNY (2012) Frictional crack initiation and propagation analysis using the numerical manifold method. Comput Geotech 39(1):38–53

Wu W, Yang Y, Zheng H (2020) Enriched mixed numerical manifold formulation with continuous nodal gradients for dynamics of fractured poroelasticity. Appl Math Model 86:225–258

Xu D, Wu A, Yang Y, Lu B, Liu F, Zheng H (2020) A new contact potential based three-dimensional discontinuous deformation analysis method. Int J Rock Mech Min Sci 127:104206

Yang Y, Chen T, Zheng H (2020a) Mathematical cover refinement of the numerical manifold method for the stability analysis of a soil-rock-mixture slope. Eng Anal Bound Elem 116:64–76

Yang Y, Guo H, Xiaodong F, Zheng H (2018a) Boundary settings for the seismic dynamic response analysis of rock masses using the numerical manifold method. Int J Numer Anal Methods Geomech 42(9): 1095–1122

Yang Y, Sun G, Zheng H (2019b) Modeling unconfined seepage flow in soil-rock mixtures using the numerical manifold method. Eng Anal Bound Elem 108:60–70

Yang Y, Sun G, Zheng H (2019b) Stability analysis of soil-rock-mixture slopes using the numerical manifold method. Eng Anal Bound Elem 109:153–160

Yang Y, Sun G, Zheng H (2020b) A high-order numerical manifold method with continuous stress/strain field. Appl Math Model 78: 576–600

Yang Y, Sun Y, Sun G, Zheng H (2019d) Sequential excavation analysis of soil-rock-mixture slopes using an improved numerical manifold method with multiple layers of mathematical cover systems. Eng Geol 261:105278

Yang Y, Sun G, Zheng H, Yan C (2020c) An improved numerical manifold method with multiple layers of mathematical cover systems for the stability analysis of soil-rock-mixture slopes. Eng Geol 264: 105373

Yang Y, Wu W, Zheng H, Liu X (2020d) A high-order three dimensional numerical manifold method with continuous stress/strain field. Eng Anal Bound Elem 117:309–320

Yang Y, Xu D, Zheng H (2018c) Explicit discontinuous deformation analysis method with lumped mass matrix for highly discrete block system. Int J Geomech 18(9):04018098

Yang Y, Zheng H (2016) A three-node triangular element fitted to numerical manifold method with continuous nodal stress for crack analysis. Eng Fract Mech 162:51–75

Yang Y, Zheng H (2017) Direct approach to treatment of contact in numerical manifold method. Int J Geomech 17(5):E4016012

Yang Y, Zheng H, Sivaselvan MV (2017) A rigorous and unified mass lumping scheme for higher-order elements. Comput Methods Appl Mech Eng 319:491–514

Yang YT, Tang XH, Zheng H, Liu QS, He L (2016) Three-dimensional fracture propagation with numerical manifold method. Engineering Analysis with Boundary Elements 72:65–77

Yang YT, Tang XH, Zheng H, Liu QS, Liu ZJ (2018b) Hydraulic fracturing modeling using the enriched numerical manifold method. Appl Math Model 53:462–486

Yang YT, Sun GH, Zheng H (2019a) Investigation of the sequential excavation of a soil-rock-mixture slope using the numerical manifold method. Eng Geol 256:93–109

Zheng H, Yang Y (2017) On generation of lumped mass matrices in partition of unity based methods. Int J Numer Methods Eng 112(8):1040–1069

Zheng H, Xu DD (2014) New strategies for some issues of numerical manifold method in simulation of crack propagation. Int J Numer Methods Eng 97(13):986–1010

Zheng H, Li CG, Lee CF, Ge X (2002) Finite element method for solving the factor of safety. Chinese Journal of Geotechnical Engineering 24(5):626–628

Zheng H, Liu DF, Li CG (2005) Slope stability analysis based on elasto-plastic finite element method. Int J Numer Methods Eng 64(14): 1871–1888

Zhuang X, Augarde CE, Mathisen KM (2012) Fracture modeling using meshless methods and level sets in 3D: framework and modeling. Int J Numer Methods Eng 92:969–998

Zienkiewicz OC, Taylor RL (2000) The finite element method, 5th edn. Butterworth-Heinemann, Oxford